

Study of Structural, Electrical and Magnetic Properties of Manganese Doped Cobalt Ferrite Nanoparticles with Non-stoichiometric Composition

M. Z. Ahsan^{1,2} and F. A. Khan²

1. Department of Physics, Military Institute of Science and Technology (MIST), Dhaka-1216, Bangladesh

2. Department of Physics, Bangladesh University of Engineering and Technology (BUET), Dhaka-1000, Bangladesh

Abstract: The nanoparticles of $\text{Co}_{1+x}\text{Mn}_x\text{Fe}_{2-x}\text{O}_4$ ($0 \leq x \leq 0.5$) ferrite system are synthesized by solid-state reaction route using planetary ball milling technique to investigate structural, electrical and magnetic properties. The X-ray diffraction patterns confirm the inverse spinel structure with residual oxide phases. Three distinct regions of frequency response on dielectric constant are observed $\text{Co}_{1.25}\text{Mn}_{0.5}\text{Fe}_{1.75}\text{O}_4$ as determined by the Wayne Kerr Impedance Analyzer. The first two regions of frequency response 1.13-4.5 MHz and 4.5-6.5 MHz exhibit the normal behavior but the last region 6.5-10.5 MHz indicates its anomalous behavior due to concurrent contribution of O^{2-} , Fe^{3+} , Co^{2+} and Mn^{3+} ions in the relaxation process for sintering effects (sintered at 700 °C). This anomalous behavior is found to be pronounced and significant for the sample of composition $\text{Co}_{1.25}\text{Mn}_{0.25}\text{Fe}_{1.75}\text{O}_4$, which may be suitable to be used in the frequency band filter over wide range of frequencies. The single peak of imaginary part of dielectric constant (ϵ'') indicates that the conduction process in this sample is due to the grain boundary resistance. The pronounced increase of capacitance (C) as observed from 100 °C to 125 °C in temperature dependent measurement (30-125 °C) is expected to cause from the change of polarization across the grain boundary due to redistribution of ions by the thermal agitation. The variation of resistance (R) with temperature (30-125 °C) is found to exhibit semiconducting behavior that resulted from the p-type carriers ($\text{Co}^{2+}/\text{Co}^{3+}$). A significant increase of Z from 105 °C with the increase of temperature indicates the signature of phase transition from ferrimagnetic-to-ferromagnetic, which may be ascribed to the increase of Co content. The appearance of the single semicircular arc in the Cole-Cole plot may be attributed to the contribution of grain boundary resistance and correspond to the parallel equivalent circuit of resistor-capacitor (R-C) combination with single relaxation time. Saturation magnetization of $\text{Co}_{1.25}\text{Mn}_{0.25}\text{Fe}_{1.75}\text{O}_4$ and $\text{Co}_{1.375}\text{Mn}_{0.375}\text{Fe}_{1.625}\text{O}_4$ is found to be greater than the literature value (61.5 emu/g) of un-doped cobalt ferrite in the measurement of their initial magnetization using Lakeshore vibrating sample magnetometer. The negative real part of AC permeability of $\text{Co}_{1.5}\text{Mn}_{0.5}\text{Fe}_{1.5}\text{O}_4$ signifies the diamagnetic behavior in the frequency range 0.13-25.2 MHz and expected to cause from the formation of magnetic dipoles opposite to the applied field due to Mn^{2+} in the B site. The samples are expected to be suitable for dielectric heating and high frequency applications.

Key words: Cobalt ferrite, dielectric constant, capacitance, resistance, impedance, cole-cole plot, magnetization.

1. Introduction

Cobalt ferrites are reported as the best example of the hard ferrite materials because of their excellent chemical stability, mechanical hardness, and reasonable saturation magnetization and high magneto crystalline anisotropy [1]. They are now being used in high-density recording media, ferro-fluids, MRI

(magnetic resonance imaging), biomedical diagnostics, radio frequency hyperthermia and drug delivery as reported elsewhere in literatures [1-6]. Cobalt ferrite is of inverse spinel structure where relatively larger oxygen ions (O^{2-}) form cubic closed pack (ccp) lattice. It's tetrahedral (A) and octahedral (B) sites formed by the oxygen ions (O^{2-}) are occupied by metal ions (Fe^{3+} and Co^{2+} ions). A site is occupied by Fe^{3+} ions and B site by Fe^{3+} and Co^{2+} ions in equal proportionate. Recently, Cobalt ferrites doped with metallic ions

Corresponding author: M. Z. Ahsan, master, professor, research fields: magnetism and advanced magnetic materials.

have received renewed attention across the world to optimize them both in sensor and high frequency applications. These applications are mostly based on structural, magnetic and electrical behaviors and their alteration or tuning by adjusting substitution level of dopants, sintering temperature and their particle size. As such efforts have already been made to substitute Co or Fe by metal ions for offering the ability to tailor the structural, magnetic and electrical properties in controlled manner.

The dielectric constant of $\text{CoDy}_x\text{Fe}_{1-x}\text{O}_4$ is reported to decrease with the increase of frequency in the low frequency range which is the normal behavior [7]. In the low frequency range, the dielectric constant of $\text{CoZn}_x\text{Fe}_{1-x}\text{O}_4$ is found to decrease significantly with the increase of Zn concentration where Zn replaced Fe as reported in literature [8]. In the frequency range from 20 Hz to 1 MHz, the dielectric constant dispersion of $\text{CoFe}_{2-x}\text{Mn}_x\text{O}_4$ fits to the modified Debye's function with more than one ion contributing to the relaxation, where the relaxation time and spread factor found to be $\sim 10^{-4}\text{s}$ and $\sim 0.35(\pm 0.05)$ respectively as exhibited in literature [9]. The dielectric properties are strongly affected by the cation redistributions with the increase of Mn concentration in $\text{Co}_{1-x}\text{Mn}_x\text{Fe}_2\text{O}_4$ as well as improved their resistive property, which make them attractive for high frequency applications as reported in literature [10]. Besides the ferri-ferromagnetic Curie temperature is found to be tunable by changing Mn content in $\text{Co}_{1-x}\text{Mn}_x\text{Fe}_2\text{O}_4$ and their AC electrical property is also strongly frequency dependent as presented in literature [11]. The frequency dependent AC impedance measurement of $\text{CoMn}_x\text{Fe}_{2-x}\text{O}_4$ makes possible to use it infrequency band filter design as demonstrated in literature [12]. Low level ($x = 0.1$ and 0.2) substitution of Mn in $\text{CoFe}_{2-x}\text{Mn}_x\text{O}_4$ induces a residual phase Fe_2O_3 and MnO_2 , and increases the density of intergranular pores and the grain size but further increase of Mn concentration decreases the grain size

with the same porosity as reported in literature [13]. The formation of two phases for $x > 1$ in the non-stoichiometric compound $\text{Co}_x\text{Fe}_{3-x}\text{O}_4$ ($x = 1$ to 2) is observed, where the coercivity increases but magnetization decreases with the increase of Co concentration and also reported about the influence of deviation from the stoichiometric on their overall properties [14]. Keeping these in view and as subsequent effort, a system of cobalt ferrite with non-stoichiometric

composition $\text{Co}_{1+x}\text{Mn}_x\text{Fe}_{2-x}\text{O}_4$ where $x = 0.25, 0.375, 0.5$ have been synthesized through solid state reaction route using planetary ball milling technique and reporting some of their structural, electrical and magnetic properties in this paper, which may open up a new window for dielectric heating and high frequency applications.

2. Experimental

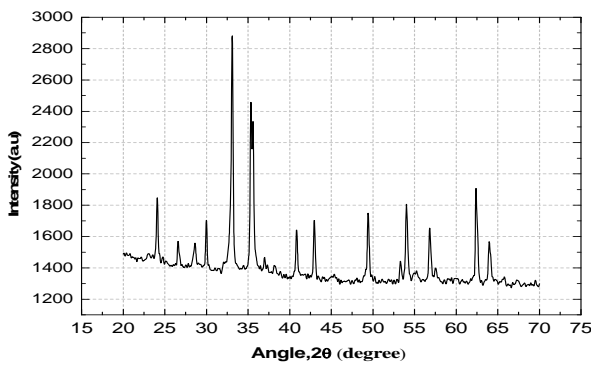
The sample for the present work has been prepared by the solid state reaction route using the planetary ball milling technique. The powder of Co_2O_3 , MnO_2 and Fe_2O_3 were mixed in desired proportionate and hand milled for 2 hours before calcination. After calcination at 550°C , again the mixer was ball milled for 12 hours. The non-stoichiometric compositions of the prepared sample were $\text{Co}_{1.25}\text{Mn}_{0.25}\text{Fe}_{1.75}\text{O}_4$, $\text{Co}_{1.375}\text{Mn}_{0.375}\text{Fe}_{1.625}\text{O}_4$ and $\text{Co}_{1.5}\text{Mn}_{0.5}\text{Fe}_{1.5}\text{O}_4$. Afterwards, disc shaped (tablet) sample of $\text{Co}_{1.25}\text{Mn}_{0.25}\text{Fe}_{1.75}\text{O}_4$ was made by hydraulic pressing machine at pressure 5,000 PSI and sintered at temperature 700°C for the dielectric measurement and in the similar way toroid shaped sample of $\text{Co}_{1.5}\text{Mn}_{0.5}\text{Fe}_{1.5}\text{O}_4$ was made for AC permeability measurement. In order to analyze the structural parameters, X-ray diffraction of the sample $\text{Co}_{1.25}\text{Mn}_{0.25}\text{Fe}_{1.75}\text{O}_4$ was taken with $\text{Cu-K}\alpha$ radiation ($\lambda = 1.54 \text{ \AA}$) by the X-ray diffractometer at Bangladesh University of Engineering and Technology (BUET). The scanning angular range (2θ) was between 10° and 80° . The Wayne Kerr

Impedance Analyzer 6,500 B series used to measure dielectric constant, capacitance, impedance and resistance of the sample $\text{Co}_{1.25}\text{Mn}_{0.25}\text{Fe}_{1.75}\text{O}_4$ and AC permeability of $\text{Co}_{1.5}\text{Mn}_{0.5}\text{Fe}_{1.5}\text{O}_4$ in the frequency range 100 Hz to 120 MHz at spot (room) temperature 30 °C. Both the frequency and temperature dependent measurements were performed of the sample $\text{Co}_{1.25}\text{Mn}_{0.25}\text{Fe}_{1.75}\text{O}_4$. The temperature range was 30 °C to 125 °C for temperature dependent measurement of capacitance (C), impedance (Z) and resistance (R) at spot frequency 1.3 MHz. Initial magnetization for samples of compositions $\text{Co}_{1.25}\text{Mn}_{0.25}\text{Fe}_{1.75}\text{O}_4$ and $\text{Co}_{1.375}\text{Mn}_{0.375}\text{Fe}_{1.625}\text{O}_4$ was measured using Lakeshore VSM (vibrating sample magnetometer) to analyze the effect of Mn content there on for the purpose.

3. Result and Discussion

3.1 Structural Properties

Fig. 1a shows the XRD pattern of $\text{Co}_{1.25}\text{Mn}_{0.25}\text{Fe}_{1.75}\text{O}_4$, which confirms the formation of inverse spinel structure of the sample $\text{Co}_{1.25}\text{Mn}_{0.25}\text{Fe}_{1.75}\text{O}_4$ with residual oxide phases. It can be seen from the XRD pattern that the peaks at 30°, 33°, 43°, 53°, 57° and 62° corresponds to the crystal planes of (220), (311), (400), (422), (511) and (440) of the sample, which are in good agreement with already reported literatures [5-7]. The other peaks at 30°, 49°, 54°, 64° correspond to Fe_2O_3 , at 37°, 56° to



MnO_2 and at 35°, 37°, 38°, 46°, 55°, 65° to Co_2O_3 residual oxide phases, which are almost in agreement to the reported literatures [15-18]. Williamson-Hall plot as shown in Fig. 1b has been used to determine the crystallite size. The crystal plane (311) has been used to calculate the lattice constant (a). The Stanley's equations have been used to evaluate tetrahedral and octahedral hopping and bond lengths using this calculated a (8.492 Å). Besides the X-ray density (ρ_x) and porosity of the sample have been calculated using the formula $\rho_x = \frac{8M}{Na^3}$ and $P\% = 1 - \frac{\rho_x}{\rho_b}$ respectively. The values of all these structural parameters along with their corresponding literature values [5] as well as theoretical values [19] are tabulated in Table 1, which exhibits that the experimental values are almost matched with the literature and theoretical values.

3.2 Frequency Dependent Dielectric Constant of $\text{Co}_{1.25}\text{Mn}_{0.25}\text{Fe}_{1.75}\text{O}_4$

Fig. 2a shows the frequency dependent real part of dielectric constant (ϵ') measured at room temperature for the sample of composition $\text{Co}_{1.25}\text{Mn}_{0.25}\text{Fe}_{1.75}\text{O}_4$. It is observed that ϵ' is strongly dependent on the frequency. A sharp increase of ϵ' is found at 1.3 MHz for the sample, which may be due to the contribution of all the four types of mechanism of polarization (electronic, ionic, dipolar and interfacial). Afterwards, ϵ' is observed to decrease rapidly with

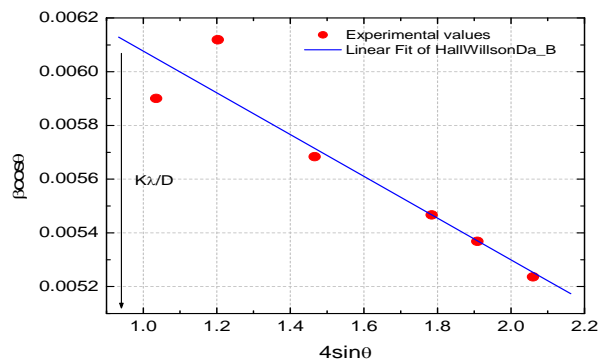


Fig. 1 (a) X-ray diffraction pattern; (b) Williamson-Hall Plot.

Table 1 Structural parameters of $\text{Co}_{1.25}\text{Mn}_{0.25}\text{Fe}_{1.75}\text{O}_4$ and comparison with literature and theoretical values.

Parameters	Experimental values	Literature values [5]	Theoretical values [19]
Crystallite size: Williamson – Hall plot	22.51 nm	14.33 nm	-
Lattice constant, $a = d_{hkl}\sqrt{h^2 + k^2 + l^2}$	8.492 Å	8.439 Å	8.386 Å
Tetrahedral hopping length, $L_A = \frac{a\sqrt{3}}{4}$	3.677 Å	3.654 Å	3.631 Å
Octahedra hopping length, $L_B = \frac{a\sqrt{2}}{4}$	3.002 Å	2.983 Å	2.965 Å
Tetrahedral bond length, $A - O = \left(u - \frac{1}{4}\right)a\sqrt{3}$ Å	1.839 Å	1.914 Å	1.816 Å
Octahedral bond length, $B - O = \left(\frac{5}{8} - u\right)a$ Å	2.123 Å	2.060 Å	2.096 Å
X-ray density, $\rho_x = \frac{8M}{Na^3}$	4.910 g/cm ³	5.167 g/cm ³	5.609 g/cm ³
Porosity, $P\% = 1 - \frac{\rho_x}{\rho_b}$	12.46%	-	-

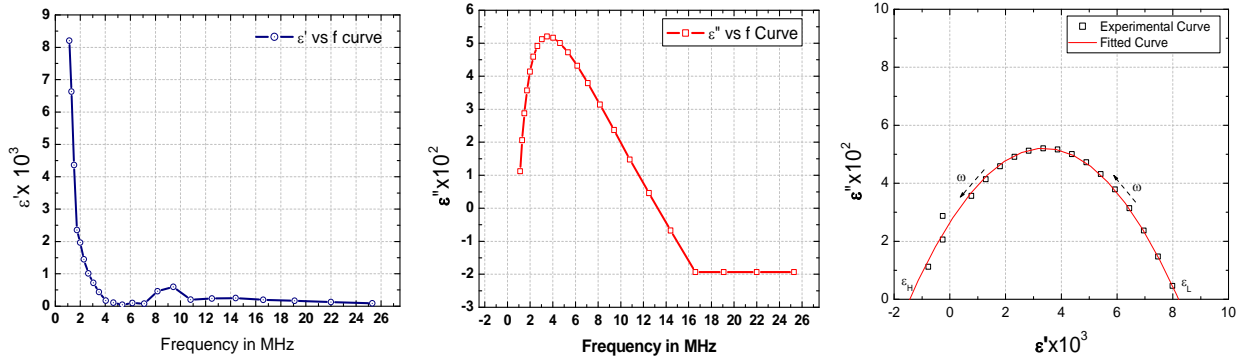


Fig. 2 (a) ϵ' vs. f curve; (b) ϵ'' vs. f curve; (c) Cole-Cole plot of complex permittivity.

the increase of frequency and remains constant from 4.5 MHz to 6.5 MHz. The decrease of ϵ' is expected to arise from the transition of interfacial polarization to dipolar polarization as explained in literature [20]. The constancy of ϵ' between 4.5 and 6.5 MHz is due to the absence of three sources of polarization and presence of the mechanism of electronic polarization as reported in literature [21]. The electronic polarization is found to be almost independent of frequency. The hump is observed in 6.5-10.5 MHz indicates a secondary frequency response of ϵ' and may have been originated from the ionic and orientation polarizations across the grain boundaries. The dispersion of ϵ' in this frequency range may be attributed to the concurrent contribution of O^{2-} , Fe^{3+} , Co^{2+} and Mn^{3+} ions in the relaxation process due to sintering effects as explained in literature [22]. So, three distinct regions of frequency response on ϵ' are observed; such as 1.13-4.5 MHz, 4.5-6.5 MHz and 6.5-10.5 MHz. The earlier two demonstrate the

normal behavior of ϵ' . The last one (6.5-10.5 MHz) indicates its anomalous behavior, which may be suitable for the frequency band filter design. Fig. 2b depicts the variation of imaginary part of dielectric constant (ϵ'') with the increase of frequency, which is a measure of energy loss within the dielectric medium and is known as dielectric loss factor. The appearance of single peak of ϵ'' at 3.47 MHz (snap shot) means that the conduction process in the sample is due to the grain resistance only that corresponds to the maximum energy loss as heat and may make it suitable for dielectric heating applications. Afterwards ϵ'' is found to decrease almost linearly with the increase of frequency up to 16.66 MHz (snap shot) and then become independent of frequency. The decrease of ϵ'' is expected to cause from the decrease of the dipole orientation (relaxation) as reported in literature [23] and the constancy may be attributed to the electronic contribution similar to ϵ' . The Cole-Cole plot as depicted in Fig. 2c shows the dielectric

constant (ϵ') dispersion almost fits to the modified Debye's function for the sample. The appearance of the single semicircular arc may be attributed to the contribution of grain boundary resistance and correspond to the equivalent circuit of resistor-capacitor (R-C) combination in parallel as explained in literature [24] with single relaxation time. The relaxation time and spread factor obtained from ϵ' dispersion are $\sim 1.03 \times 10^{-7}$ s and ~ 0 , respectively as explained in literature [25].

3.3 Temperature Dependent Capacitance, Impedance and Resistance of $\text{Co}_{1.25}\text{Mn}_{0.25}\text{Fe}_{1.75}\text{O}_4$

Fig. 3a shows the graph for capacitance (C) as a function of temperature (30-125 °C) at frequency 1.3 MHz. The pronounced increase in C is observed from 100 °C to 125 °C with the increase of

temperature. It is expected to cause from the change of polarization of localized space charge accumulated across the grain boundaries due to redistribution of ions by the thermal agitation as reported elsewhere in literatures [26-27]. Fig. 3b shows the graphs of impedance (Z) and resistance (R) as function of temperature at spot frequency 1.3 MHz. Both the Z and R are found to decrease with increase of temperature up to 75 °C and then R become independent of temperature. The decreasing nature of variation in R may be ascribed to the semiconducting behavior and expected to arise from the p-type carriers ($\text{Co}^{2+}/\text{Co}^{3+}$) across the grain boundaries in the B site as explained in literature [28]. Besides, a significant increase of Z is noticed from 105 °C due to the slower mobility of the p-type carriers ($\text{Co}^{2+}/\text{Co}^{3+}$) compared to n-type carriers ($\text{Fe}^{2+}/\text{Fe}^{3+}$) across the grain

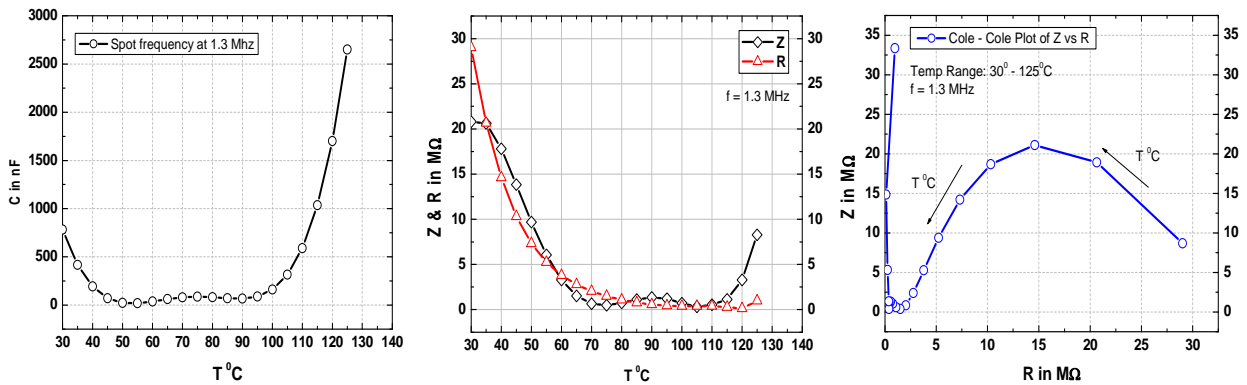


Fig. 3 (a) Capacitance as a function of temperature; (b) Impedance & resistance as a function of temperature; (c) Cole-Cole plot of Z vs. R .

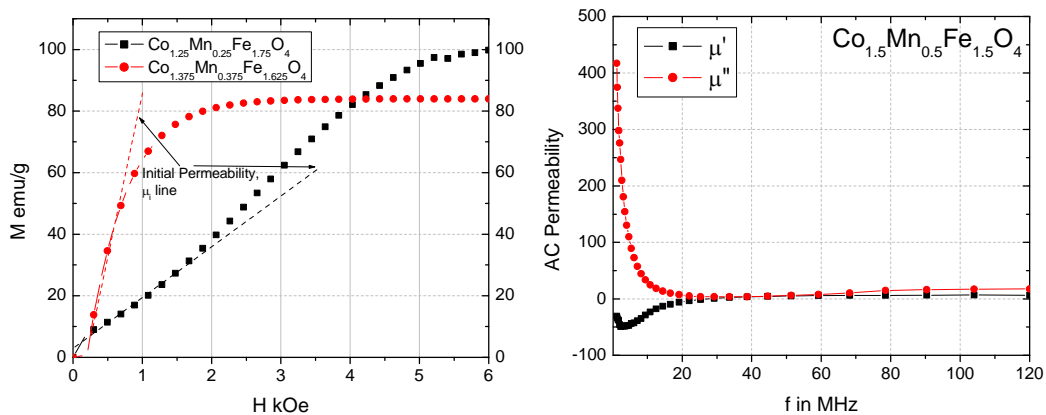


Fig. 4 (a) M-H Curves for the samples; (b) AC Permeability of $\text{Co}_{1.5}\text{Mn}_{0.5}\text{Fe}_{1.5}\text{O}_4$.

boundaries in the conduction mechanism (Verway hopping), which indicates the signature of ferrimagnetic-to-ferromagnetic transition of the sample as explained in literature [29]. The Cole-Cole plot of Z as a function of R is depicted in Fig. 3c and also confirms the contribution of grain boundary resistance. Its vertical line at a constant R exhibits the increase of impedance and conform the contribution of C ($Z = j\omega C$) in parallel combination of R-C equivalent circuit due to accumulation of localized space charge across the grain boundaries for the redistribution of ions by the thermal agitation. Moreover the decrease of the diameter of the semicircular arc of the Cole-Cole plot (Fig. 3c) while moving towards the origin with the increase of the temperature exhibits the behavior of negative temperature coefficient of resistance. This behavior also confirms the semiconducting behavior of the sample.

3.4 Magnetization and AC Permeability

Fig. 4a shows the M-H curves of initial magnetization both for the non-stoichiometric compositions $\text{Co}_{1.25}\text{Mn}_{0.25}\text{Fe}_{1.75}\text{O}_4$ and $\text{Co}_{1.375}\text{Mn}_{0.375}\text{Fe}_{1.625}\text{O}_4$. From this Fig. 4a, it is found that the saturation magnetization (M_s) decreases with the increase of Mn concentration, which may be attributed to the antiferromagnetic effect of Mn^{2+} in the B site as explained in the literature [30]. Their saturation magnetizations are found to be greater than the literature value (61.5 emu/g) [31] of the un-doped cobalt ferrite (CoFe_2O_4) at room temperature, which is expected to cause from the enhanced exchange interactions by superseding the longer hopping lengths due to the formation of residual oxide phases [18]. The initial permeability μ_i is noticed to increase with the increase of Mn content as seen from their respective slopes (slope line shown in the Fig. 4a). The higher value of μ_i for $\text{Co}_{1.375}\text{Mn}_{0.375}\text{Fe}_{1.625}\text{O}_4$ may be ascribed to the dominance of ferromagnetic effect for the ferrimagnetic-to-ferromagnetic

transition due to higher Co content in the B site, which is responsible for the overall magnetic moment in the Cobalt ferrite as explained in the literature [18]. This higher value of initial permeability μ_i makes the composition $\text{Co}_{1.375}\text{Mn}_{0.375}\text{Fe}_{1.625}\text{O}_4$ more suitable to be used in high frequency applications. Fig. 4b shows the AC response of relative permeability of the composition $\text{Co}_{1.5}\text{Mn}_{0.5}\text{Fe}_{1.5}\text{O}_4$ in the frequency range 1 to 120 MHz. From the Fig. 4b, it is seen that negative value of real part μ' of AC permeability is increasing with the increase of frequency up to 2.18 MHz (snap shot) and then decreasing up to 25.2 MHz (snap shot). After onwards it becomes positive and remains almost constant with the increase of frequency, which is normal and comes out from the contribution of the spin only orientations. The negative real part of AC permeability signifies the diamagnetic behavior in the frequency range 0.13-25.2 MHz (snap shot), which is expected to originate from the formation of magnetic dipoles opposite to the applied magnetic field due to antiferromagnetic effect of Mn^{2+} in the B site and that may correspond to the double negative media (DNG). The imaginary part μ'' of AC permeability is found to decrease with the increase of frequency due to decrease of domain wall motion and finally it becomes almost independent of frequency alike the real part, which is normal behavior that also, arises from the spin only orientations.

4. Conclusion

The 1.13-4.5 MHz, 4.5-6.5 MHz and 6.5-10.5 MHz are the three distinct regions found in the frequency dependent measurement of ϵ' at room temperature. And 1.13-4.5 MHz and 4.5-6.5 MHz regions of frequency response exhibit the normal behavior of ϵ' for the sample, 6.5-10.5 MHz region of frequency response is found to be significant and indicating its anomalous behavior. This region of frequency response found to be pronounced and thus significant for the sample, which may be suitable to be used in the frequency band filter over wide range of

frequencies. The single peak of ϵ'' at 3.47 MHz (snap shot) exhibits the conduction process in the sample is due to the grain resistance only that corresponds to the maximum energy loss as heat and may make it suitable for dielectric heating applications. The appearance of the single semicircular arc in the Cole-Cole plot may be attributed to the contribution of grain boundary resistance and correspond to the equivalent circuit of resistor-capacitor (R-C) parallel combination with single relaxation time. The pronounced variation of C with temperature is observed due to the change of polarization of localized space charge accumulated across the grain boundaries for the redistribution of ions by the thermal agitation. The nature of variation in Z and R exhibits the semiconducting behavior. A significant increase of Z with temperature from 105 °C is noticed, which indicates the signature of phase transition ferrimagnetic-to-ferromagnetic. This nature of variation of Z may be ascribed to the increase of C . The vertical line in the Cole-Cole plot of Z as a function of R conforms the contribution of C ($Z = j\omega C$) in parallel combination of R-C equivalent circuit due to accumulation of localized space charge across the grain boundaries for the redistribution of ions by the thermal agitation. The saturation magnetizations, M_s of the compositions $\text{Co}_{1.25}\text{Mn}_{0.25}\text{Fe}_{1.75}\text{O}_4$ and $\text{Co}_{1.375}\text{Mn}_{0.375}\text{Fe}_{1.625}\text{O}_4$ are found to be greater than the literature value of CoFe_2O_4 at the room temperature due to the formation of residual oxide phases and the same found to decrease with the increase of Mn^{2+} content due to its antiferromagnetic effect. The negative real part of the AC permeability is the signature of diamagnetic behavior and is expected to originate from the formation of magnetic dipoles opposite to the applied field due to Mn^{2+} in the B site. The frequency response of imaginary part of the AC permeability signifies the normal behavior. Thus the sample may be suitable to be used in dielectric heating and high frequency applications.

Acknowledgement

The authors are thankful to the ISP (International Science Programs), Uppsala University, Sweden for financial and technical support, and also to the department of physics, Bangladesh University of Engineering and Technology for experimental support.

References

- [1] Bawawaje, S., Hashi, M., and Ismail, I. 2011. "Effects of Sintering Temperature on the Grain Growth and Complex Permeability of $\text{Co}_{0.3}\text{Ni}_{0.3}\text{Zn}_{0.5}\text{Fe}_2\text{O}_4$ Material Prepared Using Mechanically Alloyed Nanoparticles." *Journal of Magnetism and Magnetic Materials* 323: 1433-9.
- [2] Ahmad, R., Gul, I. H., Zarrar, M., Anwar, H., Khan, M. B., and Khan, A. 2016. "Improved Electrical Properties of Cadmium Substituted Cobalt Ferrites Nano-particles for Microwave Application." *Journal of Magnetism and Magnetic Materials* 405 28: 28-35.
- [3] Kolekar, Y. D., Sanchez, L., Rubio E. J., and Ramana, C. V. 2014. "Grain and Grain Boundary Effects on the Frequency and Temperature Dependent Dielectric Properties of Cobalt Ferrite-Hafnium Composites." *Solid State Communications* 184: 34-9.
- [4] Sivakumar, N., Narayanasamy, A., Chinnasamy, C. N., and Jeyadevan, B. 2017. "Influence of Thermal Annealing on the Dielectric Properties and Electrical Relaxation Behaviour in Nanostructured CoFe_2O_4 Ferrite." *Journal of Physics: Condensed Matter* 19: 11.
- [5] Ponpandian, N., Balaya, P., and Narayanasamy, A. 2002. "Electrical Conductivity and Dielectric Behaviour of Nanocrystalline NiFe_2O_4 Spinel." *Journal of Physics: Condensed Matter* 14: 3221.
- [6] Singh, J. P., Kumar, H., Singhal, A., Sarin, N., Srivastava, R. C., and Chae, K. H. 2016. "Solubility Limit, Magnetic Interaction and Conduction Mechanism in Rare Earth Doped Ferrites." *Applied. Science Letters* 2 (1): 03-11.
- [7] Kumar, H., Srivastava, R. C., Singh, J. P., Negi, P., Agrawal, H. M., Das, D., and HwaChae, K. 2016. "Structural and Magnetic Properties of Dysprosium Substituted Cobalt Ferrite Nanoparticles." *Journal of Magnetism and Magnetic Materials* 401: 16-21.
- [8] Khan, A., et al. 2013. "Dielectric and Transport Properties of Zn Substituted Cobalt Ferrites." *Journal of Bangladesh Academy of Sciences* 37 (1): 73-82.
- [9] Raman, C. V., Kolekar, Y. D., Bharati, K. K., Sinha, B., and Ghosh, K. 2013. "Correlation between Structural, Magnetic and Dielectric Properties of Manganese Substituted Cobalt Ferrite." *Journal of Applied Physics*

- 114: 183907.
- [10] Atif, M., Idrees, M., Nadeem, M., Siddique, M., and Ashraf, M. W. 2016. "Investigation on the Structural, Dielectric and Impedance Analysis of Manganese Substituted Cobalt Ferrite i.e., $\text{Co}_{1-x}\text{Mn}_x\text{Fe}_2\text{O}_4$ ($0.0 \leq x \leq 0.4$).” *RSC Advances* 6: 20876-85.
- [11] Khan, A., and Feroz, Ahsan, Z. 2017. "Study of Structural and Magnetic Properties of Manganese Doped Cobalt Ferrite Nanoparticles for High Frequency and Sensor Application.” *J. Material Sci. Eng* 6: 7 (Suppl). DOI 10.4172/2169-0022-C1-079, October 19-21.
- [12] Supriya, S., Kumar, S., and Manoranjan, K. 2016. "Correlation between AC and DC Transport Properties of Mn Substituted Cobalt Ferrite.” *Journal of Applied Physics* 120: 215106.
- [13] Caltun, O. F., Rao, G. S. N., Rao, K. H., Rao, B. P., GiKim, C., Oh Kim, C., Dumitru, I., Lupu, N., and Chiriac, H. 2007. "High Magnetostrictive Cobalt Ferrite for Sensor Applications.” *Sensor Letters* 5: 1-3.
- [14] Nlebem, I. C., Moses, A. J., and Jiles, D. C. 2013. "Non-stoichiometric Cobalt Ferrite, $\text{Co}_x\text{Fe}_{3-x}\text{O}_4$ ($x = 1.0$ to 2.0) Structural, Magnetic and Magnetostrictive Properties.” *Journal of Magnetism and Magnetic Materials* 343: 49-54.
- [15] Kwan, S. K., and Yong, J. P. 2012. "Catalytic Properties of Co_3O_4 Nanoparticles for Rechargeable Li/Air Batteries.” *Nanoscale Res. Lett.* 7 (1): 47.
- [16] Edlaa, R., Gupta, S., Patel, N., Bazzanellaa, N., Fernandes, R., Kothari, D. C., and Miotelloa, A. 2016. "Enhanced H_2 Production from Hydrolysis of Sodium Borohydride Using Co_3O_4 Nanoparticles Assembled Coatings Prepared by Pulsed Laser Deposition.” *Applied Catalysis A: General*.
- [17] Pawar, R. C., Choi, D. H., and Lee, C. S. "Reduced Graphene Oxide Composites with MWCNTs and Single Crystalline Hematite Nanorhombhedra for Applications in Water Purification.” *Science Direct*. Available online at www.sciencedirect.com
- [18] Wang, H. Y., Xiao, F. X., Yu, L., Liu, B., and Lou, X. W. 2014. "Hierarchical $\alpha\text{-MnO}_2$ Nanowires @ $\text{Ni}_{1-x}\text{Mn}_x\text{O}_y$ Nanoflakes Core-Shell Nanostructures for Supercapacitors.” School of Chemical and Biomedical Engineering Nanyang Technological University 62 Nanyang Drive, Singapore 637459, Singapore.
- [19] Ahsan, M. Z., and Khan, F. A. 2017. "Study on Effects of Mn Substitution in Cobalt Ferrite.” Conference Paper, International Conference on Mechanical Engineering and Applied Science (ICMEAS) 2017, Military Institute of Science and Engineering, Mirpur Cantonment, Dhaka-1217, Bangladesh.
- [20] Khoon, T. F., Hasan, J., Wahab, Z. A., and Azis, R. S. 2016. "Electrical Conductivity and Dielectric Behavior of Manganese and Vanadium Mixed Oxide Prepared by Conventional Solid State Method.” *Engineering Science and Technology, an International Journal* 19: 2081-7.
- [21] Ahsan, M. Z., and Khan, F. A. 2016. "Dielectric Properties of $\text{Fe}_{73.5}\text{-Cu}_1\text{-Ta}_3\text{-Si}_{13.5}\text{-B}_9$ Magnetic Alloy.” *Journal of Physical Science and Application* ISSN 2159-5348. 6: 3.
- [22] Koleker, Y. D., Sanchez, L. J., and Ramana, C. V. 2014. "Dielectric Relaxation and Alternating Current Conductivity in Manganese Substituted Cobalt Ferrite.” *Journal of Applied Physics* 115: 144106.
- [23] Samy, R. A., Agami, W. R., and Eltabey, M. M. 2013. "Frequency, Temperature and Composition Dependence of Dielectric Properties of Nd^{3+} Substituted Cu-Zn Ferrites.” *Life Sci. J.* 9: 1630-4.
- [24] Bauerle, J. E. 1969. "Study of Solid Electrolyte Polarization by a Complex Admittance Method.” *J. Phys. Chem. Solids* 30: 2657-70.
- [25] Salman, F., Khalil, R., and Hazaa, H. 2014. "Dielectric Studies and Cole-Cole Plot Analysis of Silverion Conducting Glasses.” *Advance Journal of Physics Sciences* 3 (1): 1-9.
- [26] Nongjai, R., Khan, S., Asokan, K., Ahmed, H., and Khan, I. 2012. "Magnetic and Electrical Properties of In Doped Cobalt Ferrite Nanoparticles.” *Journal of Applied Physics* 112: 084321.
- [27] Farooq, H., Ahmad, M. R., Jamil, Y., Mahmood, A. H. Z., and Mahmood, T. 2012. "Structural and Dielectric Properties of Manganese Ferrite Nanoparticles.” *Journal of Basic & Applied Sciences* 8: 597-601.
- [28] Ramana, C. V., Koleker, Y. D., Bharati, K., Sinha, B., and Ghosh, K. 2013. "Correlation between Structural, Magnetic and Dielectric Properties of Manganese Substituted Cobalt Ferrite.” *Journal of Applied Physics* 114: 183907.
- [29] Ahmed, H. M. 2015. "Structural, Electric and Dielectric Properties of Cadmium Doped Nickel-Cobalt Ferrites.” *Journal of American Sciences* 11 (8).
- [30] Ovidiu Caltan, Ioan Dumitru, Marcel Feder, Nicoleta Nupu, and Horia Chiriac. 2008. "Substituted Cobalt Ferrites for Sensor Applications.” *Journal of Magnetism and Magnetic Materials* 320: e869-73.
- [31] Gul, I. H., et al. 2010. "Optical, Magnetic and Electrical Investigation of Cobalt Ferrite Nanoparticles Synthesized by Co-precipitation Route.” *Journal of Alloys and Compounds* 507: 201-6.